MOLECULAR AND CELLULAR BIOLOGY, May 1996, p. 2361–2368 Vol. 16, No. 5
0270-7306/96/$04.00+0

Rad23 Is Required for Transcription-Coupled Repair and Efficient Overall Repair in *Saccharomyces cerevisiae*

JAMES P. MUELLER AND MICHAEL J. SMERDON*

Department of Biochemistry and Biophysics, Washington State University, Pullman, Washington 99164-4660

Received 14 November 1995/Returned for modification 10 January 1996/Accepted 19 February 1996

The repair of UV-induced photoproducts (cyclobutane pyrimidine dimers) in a well-characterized minichromosome, genomic DNA, and a transcribed genomic gene (*RPB2*) of a *rad23*Δ mutant of *Saccharomyces cerevisiae* was examined. Isogenic wild-type cells show a strong bias for the repair of the transcribed strands in both the plasmid and genomic genes and efficient overall repair of both DNAs (>80% of the dimers were removed in 6 h). However, the *rad23*Δ mutant shows (i) no strand bias for repair in these genes and decreased repair of both strands, (ii) partial repair of genomic DNA (~45% in 6 h), and (iii) very poor repair of the plasmid overall (~15% in 6 h). These features, coupled with the decreased UV survival of *rad23*Δ cells, indicate that Rad23 is required for both transcription-coupled repair and efficient overall repair in *S. cerevisiae*.

Nucleotide excision repair (NER) is one of several mechanisms involved in the removal of DNA damage, including that caused by *cis-syn* cyclobutane pyrimidine dimers (CPDs) induced by UV radiation (reviewed in reference 7). It now appears that NER in chromatin may be divided into two kinetically different subpathways: one involved with repair of the overall genome (or bulk DNA) and one involved with more rapid repair of actively transcribing genes. (Note that this division is not meant to imply there are two different biochemical pathways for NER in the genome.) The latter mode has been shown for a variety of RNA polymerase II (pol II) genes and is specific for the template strand (reviewed in reference 13). This type of repair does not occur in all transcribed regions of chromatin, however. For example, repair of CPDs is very poor in each strand of the transcriptionally active fraction of ribosomal genes transcribed by RNA pol I (8). In addition, chromatin domains with high basal levels of repair (or bulk DNA repair) may not yield an obvious repair bias for strands of actively transcribed pol II genes (5, 23, 27).

The enhanced repair of transcribed strands of active pol II genes is referred to as transcription repair coupling (TRC) and appears to occur when there is an elongating pol II complex (4, 20, 38). Recent studies have demonstrated that several DNA repair proteins in yeast and mammalian cells (e.g., Rad3 and XPD) are part of the transcription factor IIH complex (reviewed in reference 7), and some of these proteins may play a role in TRC.

In *Escherichia coli*, a protein required for TRC is the product of the *mfd* gene (33). This protein displaces *E. coli* RNA polymerase that is stalled at a CPD site in vitro, allowing the (A)BC excinuclease to make incisions in the CPD-containing strand (33). This displacement may be accomplished via the Mfd protein's affinity for the UvrA subunit of the A_2B complex, which preferentially binds to damaged DNA (reviewed in reference 34), although the mechanism in vivo may be more complex (19). The *mfd* mutant shows no strand bias in the repair of transcriptionally active genes and an approximately threefold reduction in the overall removal rate of CPDs (9, 34).

A protein that seems to be involved in TRC in the yeast *Saccharomyces cerevisiae* is the product of a new gene, designated *RAD26* (41). This gene was found by homologous cloning with the human *CSB*/*ERCC6* gene being used as a probe for a yeast genomic phage library (41). In a disruption mutant of *RAD26*, a marked reduction in TRC was observed in the *RPB2* gene compared with that in wild-type (wt) cells while the removal of CPDs from the genome overall was unaffected (41). In addition, no marked increase in UV sensitivity was observed for the *rad26* cells compared with wt cells (41), similar to what is observed with *mfd* mutant cells (9, 28). Thus, it appears that *RAD26* encodes a TRC factor in *S. cerevisiae* (41).

There are several other proteins involved in but not essential for NER in *S. cerevisiae* (reviewed in reference 30). One of these is the Rad23 protein. The *RAD23* gene was cloned by Watkins et al. (46), who observed that the sequence of the amino-terminal region of the Rad23 protein is very similar to that of ubiquitin and is essential for its role in NER. This region could be substituted with the actual ubiquitin sequence, and the Rad23 protein still appeared to maintain its function in NER (46). However, this region of Rad23 does not mediate protein degradation (46), a common role of ubiquitin tagging (reviewed in reference 17). Recently, Guzder et al. (10) reported that Rad23 promotes complex formation between Rad14, a damage recognition protein (12), and the Rad25 and TFB1 components of transcription factor TFIIH. Furthermore, these authors have also reported that reconstitution of a damage-incision complex of purified yeast Rad proteins, replication protein A, and the TFIIH complex requires the Rad4-Rad23 complex (11). These observations indicate that Rad23 could play an active role in establishing the incision complex for TRC and possibly bulk repair in yeast cells.

In this study, we have examined the repair of UV-induced CPDs in a *rad23*Δ strain of *S. cerevisiae*, in which almost 90% of the *RAD23* gene is deleted by homologous recombination, and in its isogenic wt parent. Repair in a 2.6-kbp autonomously replicating plasmid (TRURAP) containing 14 nucleosomes (Fig. 1A) (40), genomic DNA, and a transcribed genomic gene (*RPB2*) was monitored. Two nucleosomes are unstable in the TRURAP minichromosome during incubation in water, the liquid-holding condition used to limit replication during repair experiments (Fig. 1A) (2). Five different transcripts are made from this plasmid at various transcription rates (Fig. 1A), though only one of these (*URA3* mRNA) appears to encode a functional protein (2, 36). Repair in TRURAP was studied by examining both the average rate of removal of CPDs from the

* Corresponding author. Phone: (509) 335-6853. Fax: (509) 335-9688.

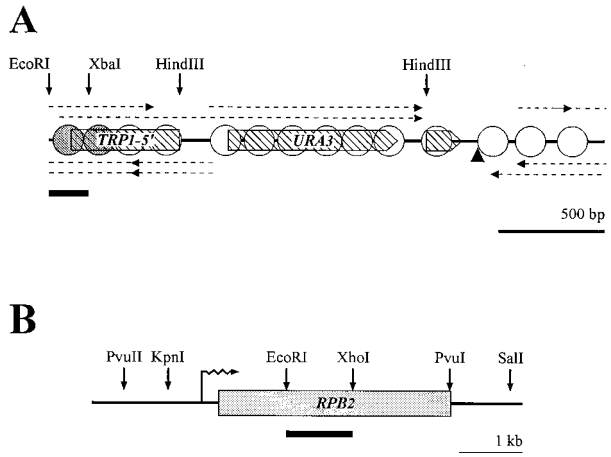

FIG. 1. Diagrams of plasmid TRURAP and the *RPB2* gene. (A) A linear representation of the yeast plasmid TRURAP, constructed by inserting the *Hin*dIII fragment of the *URA3* gene into the *Hin*dIII site of the TRP1ARS1 circle, disrupting the *TRP1* gene (40). Nucleosome positions (40) are shown as circles, with two unstable nucleosomes in water (2) being shown as stippled circles. Locations and directions of transcription (2) are indicated by dashed lines. Three transcripts go across the *Eco*RI restriction site (at the ends of the map). The *URA3* and interrupted *TRP1* genes are indicated by hatched blocks. The dark arrowhead indicates the *ARS1* site. The dark bar lying between the *Eco*RI and *Xba*I restriction sites indicates the position of the probe used for site-specific repair studies (37). (B) A map of the genomic gene *RPB2*. Transcription start and direction are indicated by the wavy arrow. The thick solid bar shows the location of the probe used for strand-specific repair studies. The sequence of this gene between the *Kpn*I and the *Sal*I sites is known (39).

entire plasmid (whole-plasmid repair) (35) and removal rates at specific CPD sites throughout the plasmid (37). The time course of whole-plasmid repair in *rad23*Δ and wt cells was compared with that of repair in the genome overall and in the essential genomic gene *RPB2* (39). There is no strand-specific repair in the *rad23*Δ strain, and there is a reduction of the repair of the nontranscribed strand and the genome overall. The results indicate that the Rad23 protein is essential for both transcription-coupled repair and efficient bulk DNA repair in *S. cerevisiae*.

MATERIALS AND METHODS

Media and strains. A minimal medium (SDM,H,W) was used in all experiments. This medium is a synthetic dextrose medium (2% dextrose and 0.67% yeast nitrogen base without amino acids [Difco]) supplemented with histidine (20 μg/ml; Sigma) and tryptophan (40 μg/ml; Sigma) (1). Strain FTY23 (*MAT*α *his3-1 trp1 ura3-52*::*URA3 gal2 gal10* [cir^0]) is *RAD* wt, and strain JMY4-23 (*MAT*α *his3-1 trp1 ura3-52*::*URA3 gal2 gal10* [cir^0] *rad23*Δ) is a *rad23*Δ isogenic mutant constructed for this study (see below). Strain JMY1-1 (*MAT***a** *his3-*Δ*1 trp1-289 ura3-52*::*URA3 rad1*Δ) is a nonisogenic *rad1*Δ strain used as a negative control. The isogenic *rad23*Δ mutant strain was constructed as previously described (26) with plasmid pDG28 (kindly provided by Louise Prakash, University of Texas, Galveston) digested with *Eco*RI. The major portion of the open reading frame of the *RAD23* gene (nucleotides +47 to +1143 [termination codon at +1193] [29a]) is replaced by a single copy of the *hisG* sequence of *Salmonella typhimurium*.

UV irradiation and repair incubation. For all experiments, cultures were grown at 30°C in SDM,H,W. UV survival and repair experiments were performed as described by Mueller and Smerdon (26). Briefly, for UV survival curves, cultures were spread on SDM,H,W plates and irradiated with a germicidal lamp (primarily at 254 nm) at various doses (measured with a Spectroline DM-254N shortwave UV meter; Spectronics Corp., Westbury, N.Y.) before incubation at 30°C in the dark. Colonies were counted after 2.5 days. For repair experiments, cells were transferred to a 50-ml centrifuge tube and pelleted. Cells were washed once, suspended in 50 ml of sterile water, and allowed to incubate for 1 h to halt cell replication (35). Cells were then poured into sterile glass petri dishes and irradiated at 25 J/m^2 before repair incubation (in the dark) for various times. Plasmid DNA was isolated as described previously (26, 35), and genomic DNA was isolated by the spheroplast method described by Mueller and Smerdon (26).

CPD analysis in DNA. CPD analyses were done as described by Mueller and Smerdon (26). Briefly, the resistance of DNA to cutting with T4 endonuclease V (T4 endo V) was monitored as a measure of repair. Resistant DNA was separated from sensitive DNA in either a neutral agarose gel (for plasmid DNA, form I and form II, respectively) or an alkaline agarose gel (for site-specific repair of TRURAP and analyses of the repair of the genome overall and the *RPB2* gene). For analysis of the *RPB2* gene, genomic DNA was first digested with *Pvu*I and *Pvu*II (38) to generate a 5.2-kb fragment encompassing the *RPB2* gene (Fig. 1B) prior to T4 endo V digestion and electrophoresis. After electrophoresis and transfer of the DNA to a nylon membrane (Hybond-N+; Amersham Corporation, Arlington Heights, Ill.), the DNA was hybridized with riboprobes made from plasmid pKS212 (Fig. 1B) (38) at 65°C in 250 mM sodium phosphate (pH 7.2)–250 mM NaCl–1 mM EDTA. Membranes were stripped in 0.4 M NaOH at room temperature before rehybridization. Autoradiograms were digitized with a Personal Densitometer SI (Molecular Dynamics, Sunnyvale, Calif.), and signals in the full-length band were determined with ImageQuaNT software (Molecular Dynamics).

RESULTS

UV survival and damage levels. The *rad23*Δ strain used in these studies was constructed by homologous recombination in which almost 90% of the open reading frame of the *RAD23* gene is replaced with a *Salmonella hisG* sequence (see Materials and Methods). We measured the survival characteristics of the *rad23*Δ strain and compared them with those of a strain lacking NER, the *rad1*Δ strain, and the isogenic wt strain. As can be seen in Fig. 2, the survival curve for the *rad23*Δ strain is intermediate to those of the wt and *rad1*Δ strains. In agreement with past reports (25, 46), this result indicates that the *RAD23* gene product is involved in but not essential for NER in *S. cerevisiae*, unlike the *RAD1* gene product (24, 47). For comparison, the survival curve of an isogenic *rad7*Δ strain is also shown in Fig. 2 (26). Remarkably, the survival curves of these two partially repair-competent strains are almost identical.

In all repair studies, CPDs were measured with T4 endo V, which makes a single-strand cut at CPDs in DNA (6). The number of nicks generated is then measured in each of the various repair assays (see Materials and Methods) (26). The

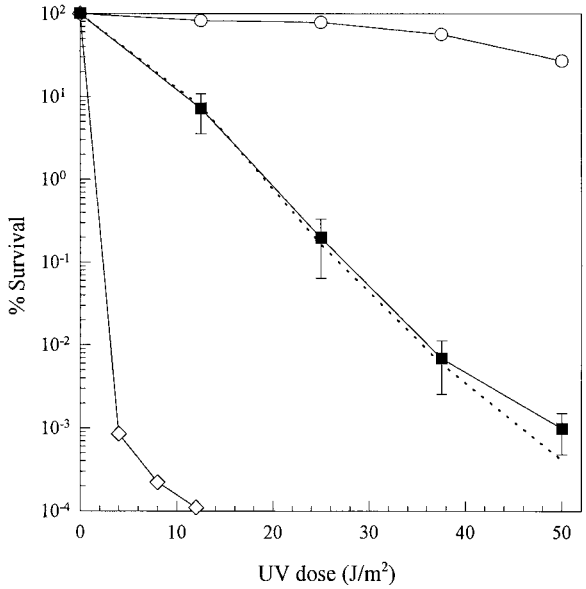

FIG. 2. UV survival curves of three yeast strains. UV survival curves were generated as previously described (26) (see also Materials and Methods). Error bars indicate standard errors of the means of three separate experiments in which an average count of three plates was taken at each time. ○, FTY23 (wt); ■, JMY4-23 (*rad23*Δ); ◇, JMY1-1 (*rad1*Δ). The dotted line is the survival curve of an isogenic *rad7*Δ strain (26).

UV dose used for most of the repair experiments (25 J/m^2) yields an average of 1.2 ± 0.2 CPDs per TRURAP plasmid (2.6 kbp) in both the *rad23*Δ and wt strains. Assuming a Poisson distribution, approximately 30% of the plasmids remain undamaged at this CPD yield. At the same dose, genomic DNA receives an average of 1.2 ± 0.2 CPDs per 5.2 kb of single-stranded DNA (i.e., 1.2 ± 0.2 CPDs per 2.6 kbp), or the same CPD yield as in TRURAP. At this level of damage, the survival of actively growing cells is ~80% for wt cells and 0.2% for *rad23*Δ cells (Fig. 2). Thus, we chose to use growth-arrested cells for our repair experiments (liquid holding), where far less cell death occurs (14) and repair measurements are not complicated by replication.

Overall repair of UV-damaged TRURAP plasmid. The overall repair of TRURAP in intact yeast cells was examined by determining the resistance of supercoiled (form I) plasmid DNA to cutting with T4 endo V as an assay for the average number of CPDs per plasmid (35). Figure 3A shows representative gels from experiments with the *rad1*Δ, *rad23*Δ, and wt strains. In the T4 endo V-treated lanes, wt cells show a decrease of nicked plasmid DNA (form II) and a concurrent increase of supercoiled plasmid DNA (form I) with repair incubation. Quantitative analysis of the photographic negatives of such gels indicates that >80% of the CPDs in TRURAP are removed (repaired) within 6 h in the wt strain (Fig. 3B). On the other hand, the *rad1*Δ strain shows no removal over the 6 h of repair incubation (Fig. 3A and B), in agreement with previous results (31, 35, 47).

The *rad23*Δ strain also shows a very low level of repair of TRURAP after 6 h (Fig. 3A). This result is surprising, since the UV survival curves (Fig. 2) predict an intermediate level of repair of the plasmid. Quantitation of several such gels indicates that ~15% of the CPDs in TRURAP are removed by the *rad23*Δ strain during this time (Fig. 3B). A similar result was observed in a different *rad23*Δ strain (i.e., different genetic background) also containing TRURAP (data not shown). Since the *rad23* and *rad7* mutants have similar survival curves (Fig. 2), the repair curve of TRURAP in a *rad7*Δ strain is also shown in Fig. 3B as a dotted line (see reference 26). The difference in repair time courses between the two mutant strains cannot be attributed to differences in CPD yield in TRURAP, since the *rad7*Δ strain also yielded 1.2 ± 0.2 CPDs per plasmid at 25 J/m^2 (26).

Repair at specific CPD sites within TRURAP. It is possible that a small number of CPD sites in TRURAP are efficiently repaired in the *rad23*Δ strain or that there is an overall loss of repair at all CPD sites. Therefore, we examined repair at 40 different CPD sites in TRURAP in this strain (see reference 37). For this assay, aliquots of supercoiled TRURAP are digested with restriction enzyme (*Eco*RI or *Xba*I) and T4 endo V before electrophoresis through an alkaline agarose gel (Materials and Methods). The DNA is transferred to a nylon membrane and probed with a short, strand-specific probe hybridizing to one end of the fragment. The short probe acts as an indirect end label for the T4 endo V-cut sites (CPDs), and the positions of these sites are obtained from the fragment sizes (37). The rate of repair at each CPD site is then obtained from the rate of decrease in band intensity (see Materials and Methods and also reference 37).

Figure 4 shows autoradiograms from such an experiment with the *rad23*Δ strain. Individual bands in each panel represent sites where unrepaired CPDs remained after each repair time. As can be seen, none of the bands disappear rapidly during the 6-h period, regardless of where they are located on TRURAP (Fig. 4; compare gels with maps between panels). Similar experiments were performed with the isogenic wt cells,

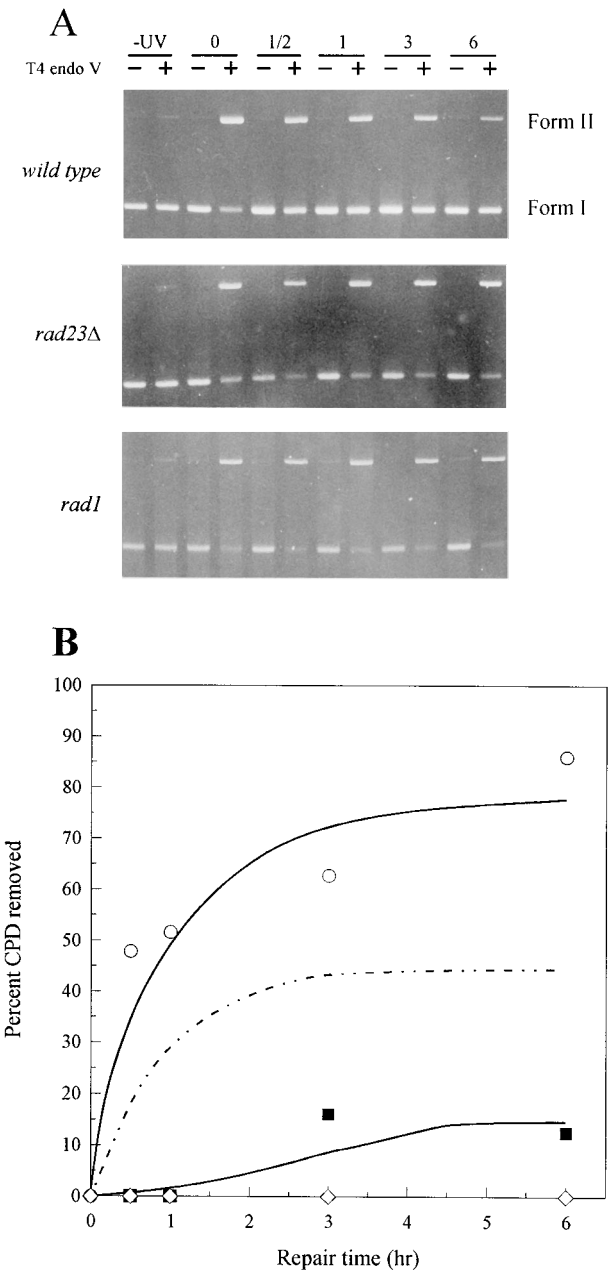

FIG. 3. Overall repair of plasmid DNA. (A) Representative gels of whole-plasmid repair experiments using three different strains. Supercoiled TRURAP was isolated after various repair times (0, 1/2, 1, 3, or 6 h) and either cut (+) or not (−) with T4 endo V. (B) Repair curves for the wt (○), *rad23*Δ (■), and *rad1*Δ (◇) strains. Datum points are averages of three or more independent experiments and were calculated as previously described (26, 35). Standard deviations ranged from ±17% for the 0.5-h time point to ±5% for the 6-h repair time. Also shown (dashed line) is the repair of TRURAP in an isogenic *rad7*Δ strain (26). The data for the wt and *rad1*Δ strains are from Mueller and Smerdon (26).

and the autoradiograms were similar to those reported previously for this strain (i.e., rapid removal of CPD bands in transcribed regions [37]). These results indicate that TRC does not occur in TRURAP in the *rad23*Δ strain.

By comparing the intensity of each band (after correction for loading) with that of its corresponding band in the no-repair lane (0 h), the rate of repair at that site can be determined (37). For example, Fig. 5A shows data for the 760- and 1,410-base

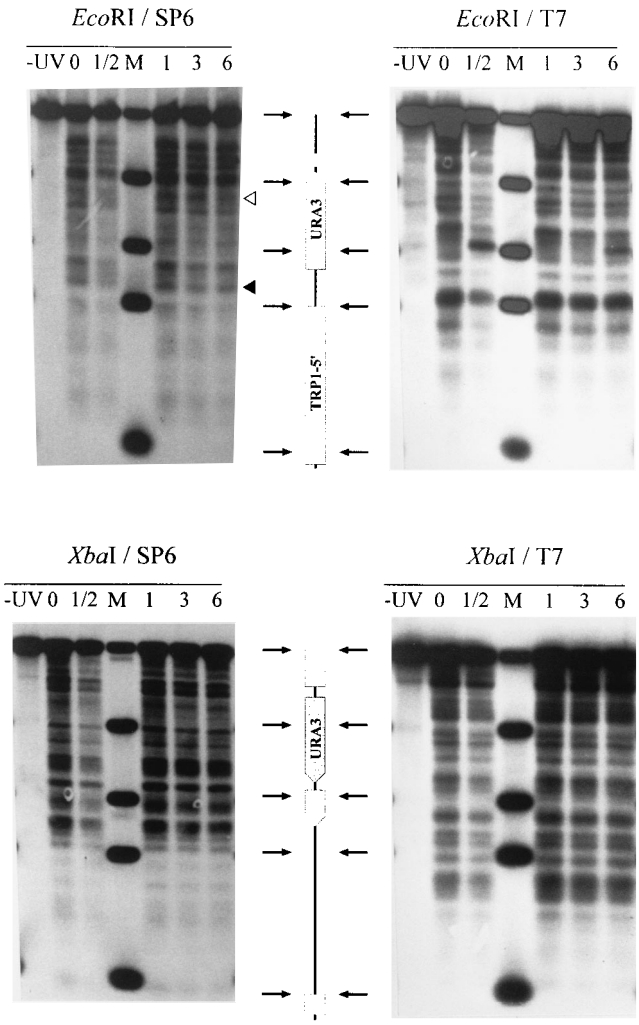

FIG. 4. Site-specific repair gels. Autoradiograms of plasmid DNA from *rad23*Δ cells that were isolated after various repair times, treated with restriction enzyme and T4 endo V, and probed with strand-specific RNA probes are shown. SP6-generated RNA probes the transcribed strand of the *URA3* gene while T7-generated RNA probes the opposite strand. Between each pair of gels is an abbreviated map of TRURAP showing the location of the *URA3* and interrupted *TRP1* genes. The arrows indicate the positions of the marker bands (M) (2,619, 1,576, 938, 615, and 186 bases [top to bottom]; see reference 37). Arrowheads next to the *Eco*RI-SP6 panel indicate the CPD sites at bases 760 (solid) and 1410 (open) used in Fig. 5A.

bands (Fig. 4 [solid and open arrowheads, respectively]) from the *Eco*RI-SP6 autoradiogram for the *rad23*Δ and wt strains. The slope of each line gives the first-order rate constant for repair at these sites (37). Note that while wt cells repair these sites quite quickly and extensively (95 and 79% after 6 h for the 760- and 1,410-base bands, respectively), the *rad23*Δ strain repairs them quite slowly. However, even though the rate of repair in the *rad23*Δ strain is quite low at these sites, there is some repair (35% for the 760-base band and 11% for the 1,410-base band) after 6 h.

Repair rate constants for 40 different CPD sites in TRU RAP for the *rad23*Δ strain and 43 sites for the wt strain were determined (Fig. 5B). Average rate constants from the *Eco*RI and *Xba*I gels are given in Fig. 5B (SP6 RNA probed on top and T7 RNA probed on bottom). At almost all sites measured on both strands, the *rad23*Δ strain shows very inefficient repair

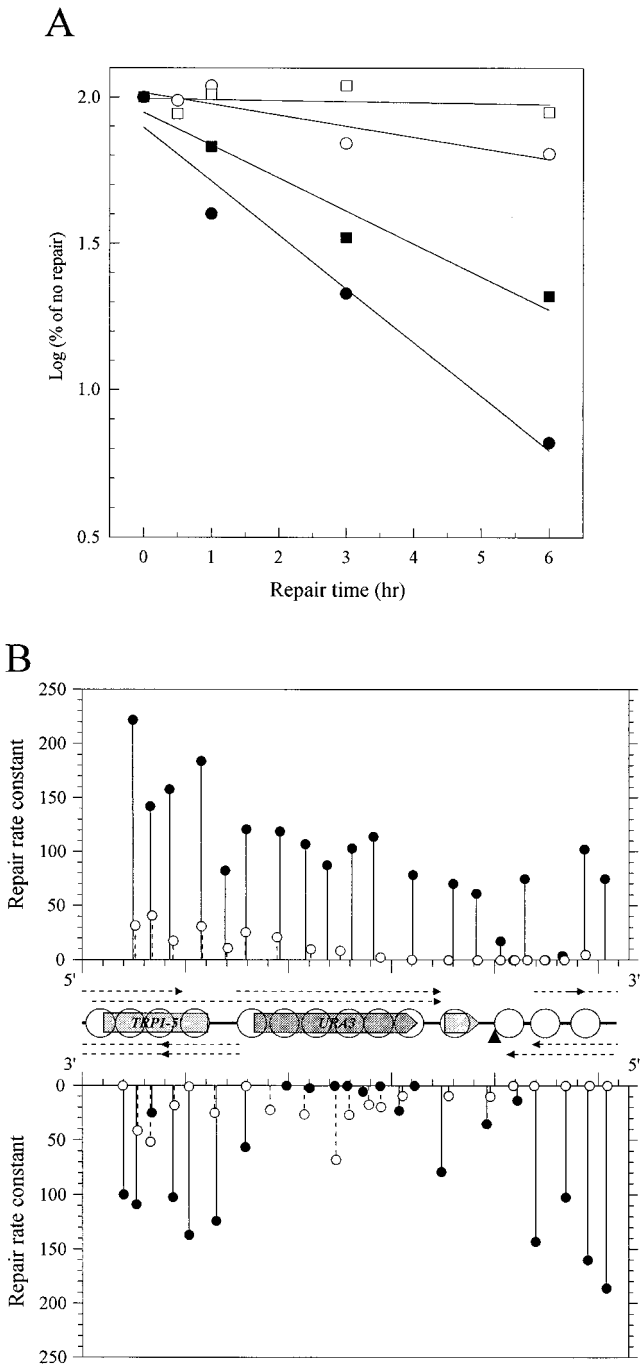

FIG. 5. Repair rates in *rad23*Δ and wt cells. (A) Generation of repair rate constants. The $\log_{10}$ of the percentage of the intensity of the no-repair sample, corrected for loading, is plotted against the repair time for the 760- (circles) and 1,410-base (squares) bands (Fig. 4). Open symbols are for the *rad23*Δ strain, and the solid symbols are for wt cells. The slopes of the linear regressions to the data (lines) were taken as first-order rate constants for those sites (37). (B) Site-specific repair map. The rate constants generated as described in the legend to panel A for 40 (*rad23*Δ; ○) and 43 (wt; ●) (26) different CPD sites in TRURAP are shown. The top panel shows data for the transcribed strand of *URA3* (SP6 RNA probed), and the bottom panel shows data for the nontranscribed strand (T7 RNA probed). Averages for the same sites and for between closely spaced sites were taken from *Eco*RI- and *Xba*I-generated data. In between the panels is a linear map of TRURAP, similar to that shown in Fig. 1A. Major tick marks on the *x* axes are 500 bases apart, starting at the *Eco*RI site.

rates compared with those of the wt strain. (A possible exception is observed at sites in the nontranscribed strand of *URA3*; however, in this region, we measured somewhat less repair in the wt strain in these experiments than we had obtained previously [37], and the very shallow slopes obtained for the repair curves [Fig. 5A] are subject to systematic error.) Furthermore, there is no apparent correlation with nucleosome position, transcribed regions (Fig. 1A and 5B), or transcription rate (2, 36). Northern (RNA) blot analysis indicates that the *rad23*Δ strain does indeed make all five RNAs from TRURAP in the same proportion as that seen in wt cells (2) following at least 3 h of repair incubation (data not shown). However, there is little (or no) strand-specific repair observed in the *rad23*Δ strain, while the wt strain clearly carries out TRC, as previously reported (37). This result is especially obvious in the region of the *URA3* gene (Fig. 5B).

Overall repair of genomic DNA. The results shown in Fig. 2 suggest that the *rad23*Δ strain should be partially competent at repairing UV-induced photoproducts. This supposition would agree with a previous report for *rad23* mutant strains that show partial repair competence in genomic DNA (25). However, since very inefficient repair occurs in the TRURAP plasmid, we examined repair of CPDs in the genome overall. For these experiments, cells were treated the same way as for the plasmid repair experiments (described above), except genomic DNA was isolated and treated with (or without) T4 endo V. The DNA was separated on alkaline agarose gels and visualized with ethidium bromide, and the number average molecular length for each sample was determined from the photographic negatives, which were calibrated for film response by an optical density step filter (see reference 26 for details). These values were used to calculate the average number of CPDs per kilobase and the extent of repair (see Materials and Methods) (26). Typical gels for these experiments are shown in Fig. 6A. In the T4 endo V-treated lanes, a shift in the intensity of the smear of DNA toward higher molecular weights indicates repair. As can be seen, this shift is visible in the gel containing DNA from wt cells (e.g., compare the lanes marked with plus signs for 0 and 6 h in the left panel of Fig. 6A). The gel from the *rad23*Δ strain (Fig. 6A, right panel) shows a lower level of repair compared with that for wt cells, evidenced by a less pronounced shift of DNA toward larger sizes.

The average number of CPDs per kilobase was determined from gel photos like those in Fig. 6A (26). As can be seen from Fig. 6B, wt cells remove over 80% of the CPDs in genomic DNA after 6 h, while the *rad23*Δ strain removes about 45% of the CPDs during this time. Conversely, the *rad1*Δ strain removes few (or no) CPDs from genomic DNA in this time period (Fig. 6B) (26), as was observed for plasmid DNA (Fig. 3) (26). For comparison, the repair curves of plasmid DNA for the wt and *rad23*Δ strains are also shown (Fig. 6B). The shaded region in Fig. 6B shows the range of fits of repair time courses for both plasmid and genomic DNA in an isogenic *rad7*Δ strain (26). As can be seen, the time courses of repair for plasmid and genomic DNA are similar for the wt, *rad1*Δ, and *rad7*Δ strains (Fig. 6B) (26). However, these curves are significantly different from that for the *rad23*Δ strain, indicating that the survival of this mutant reflects repair of CPDs in genomic DNA (see Discussion). The similarity of the genomic repair curves for the *rad7*Δ and *rad23*Δ strains explains the similarity of the UV survival curves for these strains (Fig. 2). Furthermore, sufficient levels of undamaged plasmid are present (in the dose range used in Fig. 2) to supply the required Ura3 protein in UV survival experiments (see Discussion).

Repair of *RPB2* in genomic DNA. In order to determine if the absence of TRC in TRURAP reflects a lack of TRC in the genome of the *rad23*Δ strain, we investigated repair of the constitutively expressed genomic gene *RPB2*. This gene has been used by others to monitor TRC in the yeast genome (38, 44). Once again, cells were treated as for the genomic DNA repair experiments, except genomic DNA was digested with restriction enzymes (*Pvu*I and *Pvu*II) prior to treatment with (or without) T4 endo V. The DNA was separated on alkaline agarose gels, transferred, and hybridized with a strand-specific probe for the *RPB2* gene (Fig. 1B). The CPD yield in the 5.2-kb band was measured by the method of Bohr et al. (3) to determine the extent of repair.

Typical autoradiograms for wt and *rad23*Δ cells are shown in Fig. 7A. As can be seen, the wt strain shows a marked strand

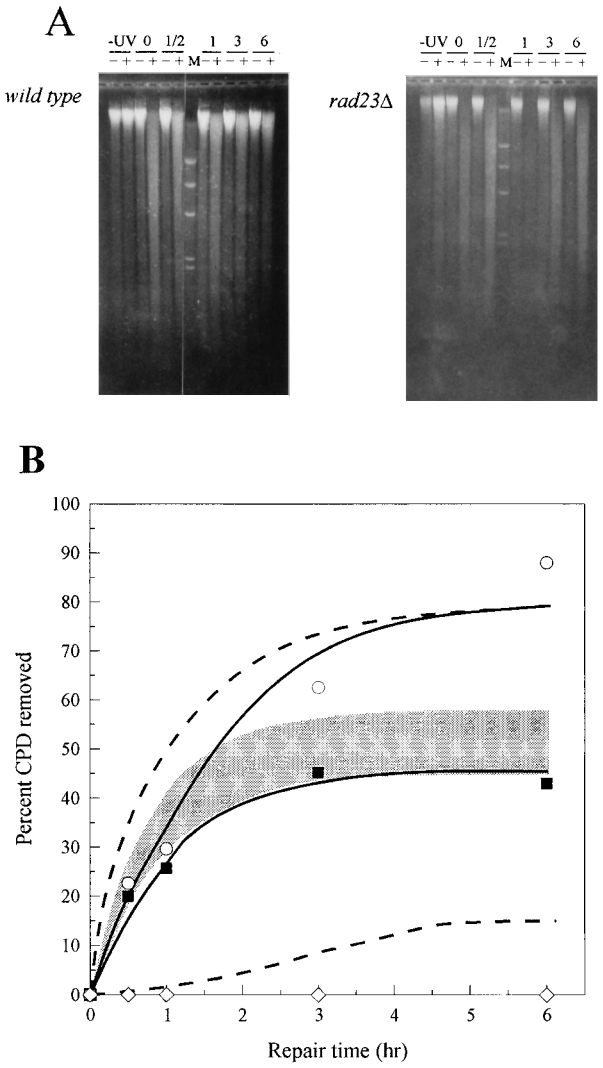

FIG. 6. Overall repair of genomic DNA. (A) Representative gels of genomic DNA that was isolated from either wt (26) or *rad23*Δ cells after various repair times (indicated in hours above the gels), treated (+) or not treated (−) with T4 endo V, and electrophoresed through alkaline agarose gels are shown. Marker (M) is phage λ DNA digested with *Hin*dIII. (B) Repair curves of genomic DNA (solid lines) determined from gels such as those shown in panel A. ○, wt cells; ■, *rad23*Δ cells; ◇, *rad1*Δ cells. (Data for wt and *rad1*Δ cells are from reference 26.) The data represent the means of three independent experiments. Standard deviations range from ±25% for the 0.5-h time point to ±8% for the 6-h repair time. Also shown are the repair curves for TRURAP in wt and *rad23*Δ cells (dashed lines [Fig. 3]) and the range of fits to genomic and plasmid repair data (shaded region) for an isogenic *rad7*Δ strain (26).

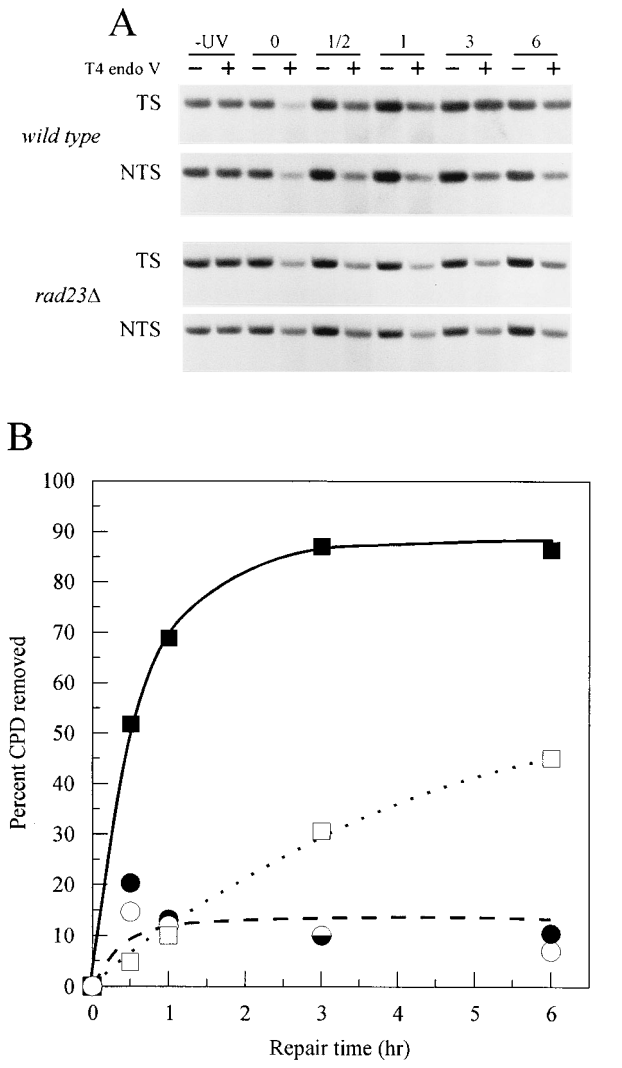

FIG. 7. Repair in the *RPB2* gene. (A) Representative autoradiograms showing the full-length, 5.2-kb DNA fragment encompassing genomic gene *RPB2*. Genomic DNA was isolated after various repair times (shown above the autoradiograms in hours), cut with *Pvu*I and *Pvu*II, and then treated with T4 endo V (+) or not treated (−). The DNA was separated on alkaline agarose gels, transferred, and hybridized with RNA probes specific for the transcribed (TS) or nontranscribed (NTS) strands. (B) Repair curves of both strands of the *RPB2* gene in wt (squares) and *rad23*Δ (circles) cells generated from autoradiograms such as those shown in panel A. Solid symbols represent data for the transcribed strand, and open symbols represent data for the nontranscribed strand (the half-solid circle is for overlapping datum points). The symbols show the averages of two (wt) or three (*rad23*Δ) independent experiments. Standard deviations for the *rad23*Δ data range from ±28% for the 0.5-h time point to ±9% for the 6-h time point.

bias in the repair of *RPB2* (Fig. 7A), in agreement with past reports (38, 44). However, for the *rad23*Δ strain (Fig. 7A), both strands of this gene appear to be repaired poorly (i.e., not very resistant to T4 endo V cutting even after 6 h). Quantitative analysis of autoradiograms such as these (3, 27) indicates that both strands of the *RPB2* gene in the *rad23*Δ strain are repaired at a low level (about 15% after 6 h), with no significant difference between the transcribed and nontranscribed strands (Fig. 7B). In contrast, wt cells remove about 85% of the CPDs from the transcribed strand, while only about 40% of the CPDs are removed from the nontranscribed strand after the same time period (Fig. 7B).

DISCUSSION

We have examined the repair of UV-induced CPDs in a minichromosome (TRURAP) and in genomic DNA in a *rad23*Δ mutant of *S. cerevisiae*. Only about 10% of the double-stranded DNA in TRURAP (and ~35% of the single-stranded DNA in TRURAP) is not transcribed, and the five different transcripts made are synthesized at different rates in wt cells (2, 36). Northern blot analysis (e.g., see reference 2) indicates that these same RNAs are made in similar proportions in the *rad23*Δ strain (data not shown). However, the mutant removes only about 15% of the CPDs in plasmid DNA after 6 h compared with >80% removed in its isogenic wt strain (Fig. 3). In contrast, the *rad23*Δ mutant removes about 45% of the CPDs from genomic DNA during this period, which is also lower than that observed for wt cells (>80% in 6 h) (Fig. 6). In addition, the *rad23*Δ mutant shows no TRC in the repair of genomic gene *RPB2*, removing only about 15% of the CPDs from each strand in 6 h compared with 85% and 40% CPDs repaired in the transcribed and nontranscribed strands, respectively, in wt cells (Fig. 7B).

The level of repair of the genome overall in the *rad23*Δ strain is consistent with the UV survival of this strain (Fig. 2). The UV survival curve of *rad23*Δ cells is very similar to that of *rad7*Δ cells (26) and lies midway between those of the wt strain and completely repair-defective strain *rad1*Δ, in agreement with past reports (24, 25, 46). In contrast to the *rad23*Δ strain, however, the *rad7*Δ strain yields similar repair curves for plasmid and genomic DNA (26) which are also similar to the curve for genomic repair in the *rad23*Δ strain (Fig. 6B). This result may be explained by consideration of the number of *URA3* genes damaged in UV-irradiated cells. Assuming a Poisson distribution, >10% of the plasmid molecules (and a larger fraction of the *URA3* genes) contain no CPDs in the UV dose range used for the survival curves (Fig. 2). Therefore, even though there is lower repair of CPDs in the plasmid compared with that in the *rad7*Δ strain, sufficient levels of undamaged *URA3* genes may exist in the plasmid population (even after an exposure of 50 J/m^2) to complement the genomic *ura3-52* defect in the *rad23*Δ cells.

The enhanced repair efficiency of CPDs in the genome of *rad23*Δ compared with that of the plasmid may reflect a difference in total transcribed regions in each (2, 16, 29) and/or differential access by repair enzymes to extrachromosomal DNA. It is interesting to note that in the *rad23*Δ mutant, the level of repair after 6 h in the two different transcribed regions studied (especially in the *RPB2* gene) is lower than both the level of repair in bulk DNA in the mutant and the nontranscribed strand of *RPB2* in the wt strain (compare Fig. 6B and 7B). It may be that an RNA polymerase stalled at a CPD site on the transcribed strand of a gene interferes with damage recognition proteins involved in bulk DNA repair because of the absence of an Mfd-like factor. If there is no dislodging of the stalled RNA polymerase, then it could prevent recognition of damage at that site by proteins scanning the DNA for lesions. Indeed, in a defined in vitro system, Selby and Sancar (32) observed that a stalled RNA polymerase inhibited the action of the (A)BC excinuclease at the polymerase-blocking CPD site. This inhibition was reversed when purified Mfd protein was added to the system (33).

The lower repair in transcribed DNA of *rad23*Δ cells may reflect an overall decrease of damage recognition and/or incision by repair proteins in this mutant. The recent report that reconstitution of a damage-incision complex of purified yeast proteins requires Rad23 supports this possibility (11). Transcription-coupled repair in the *rad23*Δ mutant could be re-

duced to a lower level of efficiency than that in the genome overall (see above). If Rad23 is also involved in the repair of bulk DNA (and nontranscribed strands of active genes), then both strands of *RPB2* would be repaired to the same low extent, as was observed (compare Fig. 6B and 7B). The rate of repair of the nontranscribed strand of *RPB2* is also lower than that of the genome overall in wt cells. Therefore, repair of the nontranscribed strand of some active genes in wt cells may be less efficient than that of the genome overall, and this difference may be maintained in *rad23*Δ cells.

Similar to our observation with *rad23* cells, van Gool et al. (41) found no significant difference in both the rates and extents of repair of CPDs in each strand of the *RPB2* gene in a *rad26* disruption mutant. However, in contrast to our results, repair of CPDs (and 6-4 photoproducts) in the genome overall was unaffected in the *rad26* strain (41). In addition, the disruption of the *RAD26* gene did not change the UV sensitivity from that of the wt strain. The data suggest that *RAD26* is the yeast equivalent of the *mfd* gene in *E. coli* (i.e., a TRC factor in yeast cells). However, since at least 40% of the genome in yeast cells is actively transcribed (e.g., see references 16 and 29), it would appear that if Rad26 is a global TRC factor (i.e., required for the repair of most transcribed genes), yeast cells are still capable of efficiently removing the bulk of the DNA damage in *rad26* cells (41). This theory would also explain the lack of effect of UV radiation on the survival of *rad26* cells (41).

It was shown that about 70% of the CPDs are repaired in both strands of the *RPB2* gene of *rad26* cells after 2 h of repair time (41) while about 15% of the CPDs were removed from each strand in the *rad23*Δ mutant (Fig. 7B). van Gool et al. (41) speculate that yeast cells have another way besides the Rad26 pathway to release a stalled RNA polymerase, such as an interaction with elongating replication enzymes, and that overall genomic repair could be unaffected by mutations in the *RAD26* gene. Thus, if replicative enzymes remove a stalled RNA polymerase, both replicative synthesis and postreplication repair could contribute to the repair they observe. A marked difference between those studies and the studies reported here is the growth conditions used. van Gool et al. (41) studied repair in actively growing *rad26* cells, whereas we examined repair in growth-arrested *rad23* cells suspended in water (35), during which the removal of CPDs occurs only through unassisted NER.

In another study, Masutani et al. (22) reported that one or possibly two human homologs to *RAD23* (*HHR23B* and *HHR23A*) are associated with a protein complex that corrects the bulk DNA repair defect of human cells from patients with xeroderma pigmentosum (complementation group C; XPC). Another protein in this complex is the product of the XPC-complementing gene (designated *XPCC*), tentatively identified as the human homolog of the yeast Rad4 protein (15, 21). These results imply that at least one of the *RAD23* homologs in humans is involved in bulk DNA repair, as this mode of NER is deficient in XPC cells (18, 42, 43). This observation also supports our earlier suggestion that Rad23 is involved in NER of the two different chromatin regions in yeast cells.

Finally, considering the similarity of the UV survival rates of the *rad7* and *rad23* strains (Fig. 2), it is interesting to note that their repair phenotypes are so different (Fig. 6B). The Rad7 protein is involved primarily in the repair of bulk DNA (26, 44, 45), whereas Rad23 affects both transcription-coupled and bulk DNA repair in *S. cerevisiae*.

ACKNOWLEDGMENTS

We thank Louise Prakash for supplying plasmid pDG28, Phillip Hanawalt for supplying plasmid pKS212, and Stephen Lloyd for supplying purified T4 endo V. We also thank members of the Smerdon laboratory and Kevin Bertrand, Antonio Conconi, Raymond Reeves, and Fritz Thoma for their stimulating and critical discussions of this work.

This study was supported by NIH grant ES02614 from the National Institute of Environmental Health Sciences.

REFERENCES

1. **Ausubel, F. M., R. Brent, R. E. Kingston, D. D. Moore, J. G. Seidman, J. A. Smith, and K. Struhl.** 1989. Current protocols in molecular biology. John Wiley & Sons, New York.
2. **Bedoyan, J., R. Gupta, F. Thoma, and M. J. Smerdon.** 1992. Transcription, nucleosome stability, and DNA repair in a yeast minichromosome. J. Biol. Chem. **267:**5996–6005.
3. **Bohr, V. A., C. A. Smith, D. S. Okumoto, and P. C. Hanawalt.** 1985. DNA repair in an active gene: removal of pyrimidine dimers from the *DHFR* gene of CHO cells is much more efficient than in the genome overall. Cell **40:** 359–369.
4. **Christians, F. C., and P. C. Hanawalt.** 1992. Inhibition of transcription and strand-specific DNA repair by α-amanitin in Chinese hamster ovary cells. Mutat. Res. **274:**93–101.
5. **de Cock, J. G. R., E. C. Klink, W. Ferro, P. H. M. Lohman, and J. C. J. Eeken.** 1992. Neither enhanced removal of cyclobutane pyrimidine dimers nor strand-specific repair is found after transcription induction of the β_3-tubulin gene in a *Drosophila* embryonic cell line *Kc*. Mutat. Res. **293:**11–20.
6. **Dodson, M. L., and R. S. Lloyd.** 1989. Structure-function studies of the T4 endonuclease V repair enzyme. Mutat. Res. **218:**49–65.
7. **Friedberg, E. C., G. C. Walker, and W. Siede.** 1995. DNA repair and mutagenesis. ASM Press, Washington, D.C.
8. **Fritz, L. K., and M. J. Smerdon.** 1995. Repair of UV damage in actively transcribed ribosomal genes. Biochemistry **34:**13117–13124.
9. **George, D., and E. M. Witkin.** 1974. Slow excision repair in an *mfd* mutant of *Escherichia coli* B/r. Mol. Gen. Genet. **133:**382–391.
10. **Guzder, S. N., V. Bailly, P. Sung, L. Prakash, and S. Prakash.** 1995. Yeast DNA repair protein RAD23 promotes complex formation between transcription factor TFIIH and DNA damage recognition factor RAD14. J. Biol. Chem. **270:**8385–8388.
11. **Guzder, S. N., Y. Habraken, P. Sung, L. Prakash, and S. Prakash.** 1995. Reconstitution of yeast nucleotide excision repair with purified Rad proteins, replication protein A and transcription factor TFIIH. J. Biol. Chem. **270:** 12973–12976.
12. **Guzder, S. N., P. Sung, L. Prakash, and S. Prakash.** 1993. Yeast DNA-repair gene *RAD14* encodes a zinc metalloprotein with affinity for ultraviolet-damaged DNA. Proc. Natl. Acad. Sci. USA **90:**5433–5437.
13. **Hanawalt, P. C.** 1995. DNA repair comes of age. Mutat. Res. **336:**101–113.
14. **Haynes, R. H., and B. A. Kunz.** 1981. DNA repair and mutagenesis in yeast, p. 371–414. *In* J. N. Strathern, E. W. Jones, and J. R. Broach (ed.), The molecular biology of the yeast *Saccharomyces*: life cycle and inheritance. Cold Spring Harbor Laboratory, Cold Spring Harbor, N.Y.
15. **Henning, K. A., C. Peterson, R. Legerski, and E. C. Friedberg.** 1994. Cloning the *Drosophila* homolog of the xeroderma pigmentosum complementation group C gene reveals homology between the predicted human and *Drosophila* polypeptides and that encoded by the yeast *RAD4* gene. Nucleic Acids Res. **22:**257–261.
16. **Herefored, L., and M. Rosbash.** 1977. Number and distribution of polyadenylated RNA sequences in yeast. Cell **10:**453–462.
17. **Jentsch, S.** 1992. The ubiquitin-conjugation system. Annu. Rev. Genet. **26:** 179–207.
18. **Kantor, G. J., L. S. Barsalou, and P. C. Hanawalt.** 1990. Selective repair of specific chromatin domains in UV-irradiated cells from xeroderma pigmentosum complementation group C. Mutat. Res. **235:**171–180.
19. **Kunala, S., and D. E. Brash.** 1995. Intergenic domains of strand-specific repair in *Escherichia coli*. J. Mol. Biol. **246:**264–272.
20. **Leadon, S. A., and D. A. Lawrence.** 1991. Preferential repair of DNA damage on the transcribed strand of the human metallothionein genes requires RNA polymerase II. Mutat. Res. **255:**67–78.
21. **Legerski, R., and C. Peterson.** 1992. Expression cloning of a human DNA repair gene involved in xeroderma pigmentosum group C. Nature (London) **359:**70–73.
22. **Masutani, C., K. Sugasawa, J. Yanagisawa, T. Sonoyama, M. Ui, T. Enomoto, K. Takio, K. Tanaka, P. J. van der Spek, D. Bootsma, J. H. J. Hoeijmakers, and F. Hanaoka.** 1994. Purification and cloning of a nucleotide excision repair complex involving the xeroderma pigmentosum group C protein and a human homologue of yeast RAD23. EMBO J. **13:**1831–1843.
23. **Mauldin, S. K., T. M. Freeland, and R. A. Deering.** 1994. Differential repair of UV damage in a developmentally regulated gene of *Dictyostelium discoideum*. Mutat. Res. **314:**187–198.

24. **McCready, S. J., J. M. Boyce, and B. S. Cox.** 1987. Excision repair in the yeast, *S. cerevisiae*. J. Cell Sci. Suppl. **6:**25–38.
25. **Miller, R. D., L. Prakash, and S. Prakash.** 1982. Defective excision of pyrimidine dimers and interstrand DNA crosslinks in *rad7* and *rad23* mutants of *S. cerevisiae*. Mol. Gen. Genet. **188:**235–239.
26. **Mueller, J. P., and M. J. Smerdon.** 1995. Repair of plasmid and genomic DNA in a *rad7*Δ mutant of yeast. Nucleic Acids Res. **23:**3457–3464.
27. **Murad, A. O., J. de Cock, D. W. Brown, and M. J. Smerdon.** 1995. Variations in transcription-repair coupling in mouse cells. J. Biol. Chem. **270:**3949–3957.
28. **Oller, A. R., I. J. Fijalkowska, R. L. Dunn, and R. M. Schaaper.** 1992. Transcription-repair coupling determines the strandedness of ultraviolet mutagenesis in *Escherichia coli*. Proc. Natl. Acad. Sci. USA **89:**11036–11040.
29. **Pérez-Ortín, J. E., E. Matallana, and L. Franco.** 1989. Chromatin structure of yeast genes. Yeast **5:**219–238.
29a. **Prakash, L.** Personal communication.
30. **Prakash, S., P. Sung, and L. Prakash.** 1993. DNA repair genes and proteins of *Saccharomyces cerevisiae*. Annu. Rev. Genet. **27:**33–70.
31. **Reynolds, R. J., and E. C. Friedberg.** 1981. Molecular mechanisms of pyrimidine dimer excision in *Saccharomyces cerevisiae*: incision of ultraviolet-irradiated deoxyribonucleic acid in vivo. J. Bacteriol. **146:**692–704.
32. **Selby, C. P., and A. Sancar.** 1990. Transcription preferentially inhibits nucleotide excision repair of the template DNA strand in vitro. J. Biol. Chem. **265:**21330–21336.
33. **Selby, C. P., and A. Sancar.** 1993. Molecular mechanism of transcription-repair coupling. Science **260:**53–58.
34. **Selby, C. P., and A. Sancar.** 1994. Mechanisms of transcription-repair coupling and mutation frequency decline. Microbiol. Rev. **58:**317–329.
35. **Smerdon, M. J., J. Bedoyan, and F. Thoma.** 1990. DNA repair in a small yeast plasmid folded into chromatin. Nucleic Acids Res. **18:**2045–2051.
36. **Smerdon, M. J., R. Gupta, and A. O. Murad.** 1993. DNA repair in transcriptionally active chromatin, p. 258–273. *In* V. A. Bohr, K. Wassermann, and K. H. Kraemer (ed.), DNA repair mechanisms. Munksgaard, Copenhagen.
37. **Smerdon, M. J., and F. Thoma.** 1990. Site-specific DNA repair at the nucleosome level in a yeast minichromosome. Cell **61:**675–684.
38. **Sweder, K. S., and P. C. Hanawalt.** 1992. Preferential repair of cyclobutane pyrimidine dimers in the transcribed strand of a gene in yeast chromosomes and plasmids is dependent on transcription. Proc. Natl. Acad. Sci. USA **89:**10696–10700.
39. **Sweetser, D., M. Nonet, and R. A. Young.** 1987. Prokaryotic and eukaryotic RNA polymerases have homologous core subunits. Proc. Natl. Acad. Sci. USA **84:**1192–1196.
40. **Thoma, F.** 1986. Protein-DNA interactions and nuclease-sensitive regions determine nucleosome positions on yeast plasmid chromatin. J. Mol. Biol. **190:**177–190.
41. **van Gool, A. J., R. Verhage, S. M. A. Swagemakers, P. van de Putte, J. Brouwer, C. Troelstra, D. Bootsma, and J. H. J. Hoeijmakers.** 1994. *RAD26*, the functional *S. cerevisiae* homolog of the Cockayne syndrome B gene *ERCC6*. EMBO J. **13:**5361–5369.
42. **Venema, J., A. van Hoffen, V. Karcagi, A. T. Natarajan, A. A. van Zeeland, and L. H. F. Mullenders.** 1991. Xeroderma pigmentosum complementation group C cells remove pyrimidine dimers selectively from the transcribed strand of active genes. Mol. Cell. Biol. **11:**4128–4134.
43. **Venema, J., A. van Hoffen, A. T. Natarajan, A. A. van Zeeland, and L. H. F. Mullenders.** 1990. The residual repair capacity of xeroderma pigmentosum complementation group C fibroblasts is highly specific for transcriptionally active DNA. Nucleic Acids Res. **18:**443–448.
44. **Verhage, R., A.-M. Zeeman, N. de Groot, F. Gleig, D. D. Bang, P. van de Putte, and J. Brouwer.** 1994. The *RAD7* and *RAD16* genes, which are essential for pyrimidine dimer removal from the silent mating type loci, are also required for repair of the nontranscribed strand of an active gene in *Saccharomyces cerevisiae*. Mol. Cell. Biol. **14:**6135–6142.
45. **Waters, R., R. Zhang, and N. J. Jones.** 1993. Inducible removal of UV-induced pyrimidine dimers from transcriptionally active and inactive genes of *Saccharomyces cerevisiae*. Mol. Gen. Genet. **239:**28–32.
46. **Watkins, J. F., P. Sung, L. Prakash, and S. Prakash.** 1993. The *Saccharomyces cerevisiae* DNA repair gene *RAD23* encodes a nuclear protein containing a ubiquitin-like domain required for biological function. Mol. Cell. Biol. **13:**7757–7765.
47. **Wilcox, D. R., and L. Prakash.** 1981. Incision and postincision steps of pyrimidine dimer removal in excision-defective mutants of *Saccharomyces*